Effect of Iron-Sulfur Cluster Environment in Modulating the Thermodynamic Properties and Biological Function of Ferredoxin from *Pyrococcus furiosus*†

Phillip S. Brereton, Marc F. J. M. Verhagen, Zhi H. Zhou, and Michael W. W. Adams*

Department of Biochemistry and Molecular Biology and the Center for Metalloenzyme Studies, University of Georgia, Athens, Georgia 30602-7229

Received November 24, 1997; Revised Manuscript Received March 23, 1998

ABSTRACT: The ferredoxin (7.5 kDa) of the hyperthermophilic archaeon, *Pyrococcus furiosus*, contains a single [4Fe-4S]$^{1+,2+}$ cluster that is coordinated by three Cys and one Asp residue rather than the expected four Cys. The role of this Asp residue was investigated using a series of mutants, D14X, where X = C, S, H, N, V, and Y, prepared by heterologous gene expression in *Escherichia coli*. While the recombinant form of the wild-type and the D14S and D14C mutants contained a [4Fe-4S]$^{1+,2+}$ cluster, the D14V, D14H, D14Y, and D14N proteins contained a [3Fe-4S]$^{0,+}$ center, as determined by visible spectroscopy and electrochemistry. The redox potentials (at pH 7.0, 23 °C) of the D14C and D14S mutants were decreased by 58 and 133 mV, respectively, compared to those of the wild-type 4Fe-ferredoxin (E_m −368 mV), while those of the 3Fe-protein mutants (including the 3Fe-form of the D14S, generated by chemical oxidation) were between 15 and 118 mV more positive than that of wild-type 3Fe-form (obtained by chemical oxidation, E_m −203 mV). The reduction potentials of all of the 3Fe-forms, except the D14S mutant, showed a pH response over the range 3.0−10.0 with a p*K* of 3.3−4.7, and this was assigned to cluster protonation. The D14H mutant and the wild-type 3Fe-proteins showed an additional p*K* (both at 5.9) assumed to arise from protonation of the amino acid side chain. With the 4Fe-proteins, there was no dramatic change in the potentials of the wild-type or D14C form, while the pH response of the D14S mutant (p*K* 4.75) was ascribed to protonation of the serinate. While the ferredoxin variants exhibited a range of thermal stabilities (measured at 80 °C, pH 2.5), none of them showed any temperature-dependent transitions (0−80 °C) in their reduction potentials, and there was no correlation between the calculated $\Delta S°'$ values and the absorbance maximum, reduction potential, or hydrophobicity of residue 14. In contrast, there was a linear correlation between the $\Delta H°'$ value and reduction potential. Kinetic analyses were carried out at 80 °C using the ferredoxin as either an electron acceptor to pyruvate oxidoreductase (POR) or as an electron donor to ferredoxin:NADP oxidoreductase (FNOR, both from *P. furiosus*). The data showed that the reduction potential of the ferredoxin, rather than cluster type or the nature of the residue at position 14, appears to be the predominant factor in determining efficiency of electron transfer in both systems. However, compared to all the variants, the reduction potential of WT Fd makes it the most appropriate protein to both accept electrons from POR and donate them to FNOR.

Cubane-type [4Fe-4S] clusters are ubiquitous in biological systems. They are found in simple redox proteins termed ferredoxins (Fds)[1] as well as in a wide range of both cytoplasmic and membrane-bound enzymes (for reviews, see refs *1*−*4*). In most systems the [4Fe-4S] cluster functions to transfer electrons and undergoes a one-electron redox couple (2+/1+) at potentials that can range from −300 to −700 mV. In addition, some Fds and some enzymes contain a [3Fe-4S]$^{+/0}$ cluster. This is a derivative of the cubane-type but has a higher potential, typically near −100 mV. While several 3Fe-clusters are known to be functional, such clusters are frequently formed by degradation of a [4Fe-4S] cluster (*5*). Another version of the cubane cluster is found in small redox proteins known as high-potential iron sulfur proteins (Hipips) which utilize a higher cluster oxidation state (3+/2+) with reduction potentials ranging from +50 to +500 mV (*6*).

For both the 4Fe- and 3Fe-type clusters, the molecular determinants of their reduction potentials within a given protein are to a large extent unknown. For the 4Fe-type, the cluster in Fds is positioned close to the surface of the protein in a hydrophilic environment, while in Hipips the cluster is buried inside the protein, surrounded by hydrophobic residues (*7*). The number of NH···S hydrogen bonds from peptide NH groups to cluster (inorganic) and/or ligand

† This research was supported by grants from the National Institutes of Health (GM-45597) and the National Science Foundation (MCB94-05783).

* Author to whom correspondence should be addressed at Department of Biochemistry, Life Sciences Building, University of Georgia, Athens, GA 30602-7229. Tel: 706 542-2060. Fax: 706 542-0229. E-mail: adamsm@bscr.uga.edu.

[1] Abbreviations: Av, *Azotobacter vinelandii*; BV, benzyl viologen; CAPS, 3-(cyclohexylamino)-1-propanesulfonic acid; CHES, 2-(*N*-cyclohexylamino)ethanesulfonic acid; DMSO, dimethyl sulfoxide; Dv, *Desulfovibrio vulgaris*; Cv, *Chromatium vinosum*; *E. coli*, *Escherichia coli*; ENDOR, electron-nuclear double resonance; EPPS, *N*-(2-hydoxyethyl)piperazine-*N*′-(3-propanesulfonic acid); Fd, ferredoxin; HEPES, *N*-(2-hydroxyethyl)piperazine-*N*′-(2-ethanesulfonic acid); Hipip, high-potential iron protein; MES, 2-(*N*-morpholino)ethanesulfonic acid; MV, methyl viologen; Pf, *Pyrococcus furiosus*; POR, pyruvate ferredoxin oxidoreductase; FNOR, ferredoxin:NADP oxidoreductase; WT, wild-type; VTMCD, variable-temperature magnetic circular dichroism.

S0006-2960(97)02864-X CCC: $15.00
Published on Web 04/29/1998

cysteinyl sulfur atoms also appears to play a role in differentiating Fd and Hipip clusters (*7, 8*). For example, the 4Fe-cluster of *Chromatium vinosum* (Cv) Hipip contains three less NH···S bonds per cluster than the clusters in four bacterial Fds. It was suggested that the increased number of NH···S bonds in Fds allows for the stabilization of the more electron-rich reduced state by removing electron density (*7*). However, further modulation of the redox potential of Fd-type 4Fe-clusters must be due to other factors. These could include the number and orientation of peptide amide groups in the vicinity of the cluster and accessibility to the cluster of solvent water molecules (*7, 9, 10*). As yet though, a molecular basis for these effects has not been elucidated.

In the present work we have utilized the Fd from the hyperthermophilic archaeon *P. furiosus* (Pf), as a model system to investigate both the molecular determinants of redox potential and the role of the protein in determining the efficiency of electron transfer between Fd and its redox partners. Pf Fd is a monomer (M_r 7500 Da) containing a single [4Fe-4S] cluster and is distinguished by its extremely high thermostability and by noncysteinyl ligation of a specific Fe site in the cluster (*11*). The typical cubane or bacterial type ferredoxin consensus sequence that is almost exclusively utilized in coordinating 4Fe- and 3Fe-clusters consists of two $CX_2CX_2CX_3CP$ motifs related by a pseudo two-fold center of symmetry between the first and second halves of the protein. Cluster ligation occurs by cysteinyl S atoms from the first three Cys residues in one motif and from the fourth Cys in the remote sequence. In 4Fe-Fds, one or more of the Cys residues in the second cluster-binding Cys motif is replaced, while the first motif maintains four Cys to bind the single cluster. With Pf Fd, however, the second Cys in the first motif (at residue 14) is also replaced, in this case by an Asp residue. Despite incomplete Cys ligation, the Pf protein contains a [4Fe-4S] cluster and the carboxylate group of Asp 14 acts as a coordinating ligand (*12*). Of all other 4Fe-Fds reported, incomplete Cys ligation has been found only in Fds I and II from *Streptomyces griseolus* where Ala replaces the second Cys (*13*). Such a substitution does not appear to stabilize a 4Fe-cluster since upon purification these proteins both contain a 3Fe-cluster.

Noncysteinyl ligation to a cubane-type FeS cluster is now known to occur in several enzymes, and in each case the anomalous cluster coordination has a functional significance. The prototypical example is the citric acid cycle enzyme, aconitase, whose 4Fe-cluster has a coordinating hydroxyl group in the absence of substrate, while binding of the carboxylate substrate results in a six coordinate Fe atom (*14*). This enzyme is representative of a large class of (de)-hydratases that utilizes a redox-inactive FeS cluster to catalyze (de)hydration reactions (*15*). In a similar vein, protonation of a non-Cys FeS cluster ligand appears to enable some proteins to couple electron and proton transfer. The double-cubane P-cluster of nitrogenase has partial serinate ligation to affect such a reaction (*16*), and the His ligands to the Rieske 2Fe-center may also allow coupled proton/electron transfer (*17*). The distal [4Fe-4S] cluster in a NiFe-hydrogenase was recently shown to be coordinated by three Cys and one His ligand, suggesting perhaps that the His has a proton-transfer role (*18*), and although structurally uncharacterized, there is evidence for noncysteinyl coordination to the novel H_2-activating FeS cluster of Fe-only hydrogenases (*19*).

Pf Fd therefore provides a much simpler model system with which to investigate the effects of noncysteinyl ligation to a cubane-type cluster. This protein also has a central position in the metabolism of Pf wherein it functions as the electron carrier for a number of oxidoreductases in both the carbohydrate (for enzymes oxidizing pyruvate and glyceraldehyde-3-phosphate, see refs *20, 21*) and peptide fermentation pathways (for enzymes oxidizing various aldehydes, formaldehyde, indolepyruvate, 2-ketoglutarate, and 2-ketoisovalerate, see refs *22*−*25*). In addition, Fd has also been shown to act as the electron donor for ferredoxin:NADP oxidoreductase (*26*). NADPH is ultimately used by hydrogenase to reduce protons to H_2 (*27*). Thus, there are a variety of oxidoreductases available with which to investigate the efficiency of Fd-enzyme interprotein electron transfer.

The remarkable stability of Pf Fd (unaffected by 12 h at 95 °C; ref *28*) also enables its redox properties to be examined over a wide range of both temperature and pH, conditions not accessible to mesophilic proteins. Indeed, for metalloproteins in general, only a limited number of thermodynamic parameters associated with electron transfer have been reported, and these are based on data obtained over a limited temperature range (*6, 29*−*33*). Similarly, previous studies on the potential correlation between thermodynamic entropy and enthalpy terms and the environment of the redox site have relied predominantly on comparing similar proteins from a variety of different organisms, e.g., with cytochrome *c* (*29*) and Hipip (*6*). The benefit of having a series of proteins differing in only one amino acid for such comparisons is obvious, and herein we present such a thermodynamic analysis for a series of Pf Fd variants, measured over a range of 80 °C.

The gene for Pf Fd was recently expressed in *E. coli* to give a recombinant protein that was indistinguishable from the wild-type (WT) Fd. In the present study a series of site-directed mutants were prepared to investigate the site-specific chemistry at position 14, the site of the cluster-coordinating Asp. Six mutants were prepared at this position (D14X; X = C, S, H, N, V, Y). Together with the 4Fe- and 3Fe-forms of the WT recombinant protein, these mutants provide an extensive set of variants to probe the effect of this position on the properties of cubane-type FeS clusters, and specifically the reduction potential, thermodynamic, and electron-transfer properties of the protein.

MATERIALS AND METHODS

Materials. Restriction enzymes, T_4 polynucleotide kinase, *E. coli* strain JM105, X-gal, and all oligonucleotides were obtained from Stratagene (La Jolla, CA). IPTG was from Alexis (San Diego, CA). Sequenase (version 2.0), ampicillin, and shrimp alkaline phosphatase were purchased from USB (Cleveland, OH). The radioactive nucleotide used for DNA sequencing was [α-^{35}S]dATP obtained from Amersham Corp (Arlington Heights, IL). The expression plasmid pTrc99A and the chromatography materials (Sephadex G-75 and Q-Sepharose Fast Flow) were from Pharmacia-LKB (Piscataway, NJ). The Mutagene kit (including the *E. coli* strains MV1190 and CJ236 and T_4 DNA polymerase and T_4 DNA ligase) was purchased from Bio-Rad (Richmond, CA). The

plasmid modified for mutagenesis was pUC118 (Worthington; Freehold, NJ). The antibiotics chloramphenicol, kanamycin monosulfate, neomycin sulfate, buffers (CAPS, CHES, MES, HEPES, and EPPS), pyruvate, benzyl viologen, methyl viologen, and metronidazole were all from Sigma (St Louis, MO). Coenzyme A was purchased from ICN (Costa Mesa, CA). The bacterial growth media (tryptone and yeast extract) were from Difco (Detroit, MI). The YM-3 ultrafiltration membranes were from Amicon (Beverly, MA). The geneclean kit was obtained from Bio 101 (Vista, CA). Al_2O_3 slurry and diamond polish were obtained from Buehler (Lake Bluff, IL).

Mutagenesis. The cloning and expression of the gene encoding Pf Fd in *E. coli* has been described previously (*34*). The *E. coli* expression system was constructed by cloning the PCR-generated Pf Fd gene fragment into the Nco1 and Sma1 sites of the vector pTrc99A. To facilitate mutagenesis, the Pf Fd gene was subcloned into a vector that can replicate in the single-stranded form, thereby allowing mutagenesis by the method of Kunkel (*35*). For this purpose the plasmid pUC118 was selected and modified to introduce a Nco1 restriction site into the 5′ end of the multiple cloning site. The modified pUC118 was prepared to enable direct ligation of the mutated Pf Fd gene from the pUC118 mutagenesis vector to the pTrc99A expression vector. The introduction of a Nco1 site into the pUC118 vector was achieved by the mutation of one base-pair using a Mutagene kit as described by the suppliers (except that chloramphenicol was not added to the liquid media during phagemid growth as it was found to inhibit production of single-stranded DNA). The sequence of the oligonucleotide used to introduce the mutation was 5′-CGA ATT CGT AAC CAT GGT CAT-3′, where the mismatched base is underlined. The mutation was confirmed by visualization on a 1% agarose-TAE gel stained with ethidium bromide after a restriction digest with Nco1. The modified plasmid was termed pUC118N.

After Nco1 and Pst1 digestion of the pUC118N plasmid and dephosphorylation with shrimp alkaline phosphatase, the plasmid was recovered and purified (Gene-clean). The WT Pf Fd gene was excised from the expression vector pAH1993 (*34*) with the same restriction enzymes (Nco1 and Pst1) and was ligated into pUC118N (*36*). The ligation reaction was used to transform *E. coli* MV1190 competent cells. Transformants were selected on LB-plates containing ampicillin, IPTG, and X-gal. Successful insertion of the Pf Fd gene was confirmed by gel analysis of a Nco1/Pst1 restriction digest. Construction of the D14N and D14Y mutants was performed using the Mutagene kit. The other mutants were prepared by PCR amplification (*37*). All mutants were confirmed by Sanger dideoxy sequencing (Sequenase kit). The Pf Fd mutant genes were subcloned into the Nco1 and Pst1 sites of the expression vector pTrc99A and used to transform *E. coli* JM105. Plasmid constructs were resequenced prior to large-scale expression to confirm that the sub-cloning step, into the expression vector, was successful.

Expression. Expression of the mutant proteins was essentially as described previously (*34*), but with the induction time increased to 12 h (*37*). Cells were grown in either 2YT, LB, or LB containing glycerol (0.5%). The cell yields were typically in the range of 7−8 g (wet weight) of cell paste/L for 2YT and LB + glycerol media and approximately 5 g/L for LB medium. Expression in *E. coli* JM105 was achieved by the addition of IPTG (1 mM) when the OD_{600} was between 0.5 and 0.6.

Purification of Fds. The mutants were purified under anaerobic conditions with all buffers containing sodium dithionite (2 mM; see ref *37*). After cell lysis (*36*) the majority of *E. coli* proteins were denatured by incubation at 70 °C for 1 h, and the extract was then placed at 4 °C overnight to further enhance precipitation of *E. coli* proteins. After centrifugation (8K rpm for 45 min; Sorvall JA-10 rotor), the supernatant was diluted 3-fold with 50 mM Tris-Cl, pH 8.0 (buffer A), and loaded onto a Q-Sepharose Fast Flow column (7 cm × 23 cm) previously equilibrated with buffer A. The column was washed with buffer A (2 L) and the absorbed proteins were eluted with a linear gradient (5 L) from 0 to 0.6 M NaCl in buffer A. Fractions containing Fd (as judged by their brown color) were pooled, concentrated by ultralfiltration (YM-3 Amicon membrane), and applied to a column (6 cm × 60 cm) of Sephadex G-75, equilibrated with buffer A at 3 mL/min. Fractions containing pure Fd as judged by electrophoretic analysis (using Tris-tricine polyacrylamide, 16% w/v ref *38*) and by the maximum value of the absorbance ratio (A_{390}/A_{280}) were combined and concentrated prior to storage under Ar at −80 °C.

UV−Visible Spectroscopy. Spectra of the oxidized and reduced form of each mutant (25−40 μM in 50 mM EPPS, pH 8.0) were recorded on a Hewlett-Packard 8452A diode array spectrophotometer at 23 °C. The proteins were reduced by the addition of sodium dithionite (3- to 5-fold molar excess over Fd) under anaerobic conditions.

Biological Assay. The ability of the Fd mutants to function as electron acceptors for Pf pyruvate ferredoxin oxidoreductase (POR; ref *20*) was determined by a direct assay as follows. The reaction mixture (2.0 mL) contained 50 mM EPPS buffer, pH 8.0, pyruvate (10 mM), coenzyme A (0.2 mM), $MgCl_2$ (1 mM), and Fd (5−125 μM). The mixture was incubated at 80 °C, and the reaction was initiated by the addition of POR (0.15 μg/mL; 18 units/mg, see below). Activity was calculated (see Results) from the decrease in absorbance at 412 nm. Curves were fitted with the Michaelis−Menten equation, and apparent K_m and V_m values were calculated. The activity of the POR was determined independently using the same assay conditions but with the artificial electron acceptor methyl viologen (1 mM) replacing Fd. One unit of POR activity catalyzed the oxidation of 1 μmol of pyruvate per min. To investigate the effect of POR concentration on specific activity, the amount of POR added to the assay was varied from 0.15 to 10 μg/mL using either WT Fd (3Fe- or 4Fe-form) or methyl viologen as the electron acceptor. POR activity using Fd as the electron acceptor was also measured by a coupled assay system using metronidazole (100 μM) to reoxidize Fd, thereby maintaining a constant amount of Fd in the mixture (*37*). The reaction conditions, apart from the addition of metronidazole and lower amounts of Fd, were identical to the uncoupled POR assay. These assays were designed such that the substrate (Fd) concentration allowed the reaction to approach V_m, i.e., $[S] \gg 5 \times K_m$. Pf POR was purified by the published procedure (*20*).

The biological activity of the Fd mutants was also assessed in a second coupled assay system in which Fd reduced by POR was subsequently oxidized by ferredoxin:NADP oxidoreductase (FNOR; ref *26*). The assay (2 mL) was

performed at 80 °C in EPPS buffer (50 mM; pH 8.0) containing pyruvate (10 mM), coenzyme A (0.2 mM), $MgCl_2$ (1 mM), Pf POR (20 μg/mL; 10 units/mg), and Fd (0.1−20 μM). The reaction was started by the addition of FNOR (5 μg/mL; 55 units/mg, see below). The reaction was followed by measuring the reduction of NADP at 365 nm. A molar absorbance of 3400 M^{-1} cm^{-1} was used for NADPH. One unit of activity in this assay is 1 μmol of pyruvate oxidized per min (equivalent to 2 μmol of Fd oxidized per min). Curves were fitted with the Michaelis−Menten equation. The activity of the FNOR was determined using the artificial electron acceptor benzyl viologen (1 mM) with NADH (0.3 mM) as the electron donor. One unit of activity of FNOR catalyzed the reduction of 2 μmol of benzyl viologen per min in CAPS buffer (50 mM, pH 10.3).

The ability of FNOR to reduce Fd mutants using NADPH as the electron donor was determined at 80 °C in 50 mM EPPS buffer, pH 8.0, containing Fd (3−75 μM), NADPH (0.3 mM), and FNOR (5 μg/mL). Fd reduction was determined by measuring the decrease in absorption at 412 nm (see Results). FNOR was purified as previously described (*26*).

Other Methods. The 3Fe-forms of both WT Fd and the D14S mutant were prepared by treatment with excess ferricyanide (*11*). The thermal stability of the Fd mutants (15 μM) was determined at 80 °C in 50 mM glycine/HCl buffer, pH 2.5. Degradation of their FeS clusters was measured by following the loss of absorption at 390 nm. Reduction potentials of the proteins and their pH dependence were measured by cyclic voltammetry at a glassy carbon electrode. The electrochemistry cell used was identical to that described by Hagen (*39*). Prior to each use, the electrode was polished with a 0.3 μm Al_2O_3 slurry and then with 1 μm diamond spray. Fd mutants (50−100 μM) in the appropriate buffer (50 mM; citrate, formate, acetate, MES, HEPES, CHES, or CAPS) containing the promoter neomycin (2 mM), added from a 20 mM stock solution in the same buffer and pH, were analyzed between pH 3.0 and 10.0 at 23 °C. The scan rate was 10 mV/s over the potential range −200 to −900 mV (versus the Ag/AgCl electrode) for the 4Fe-forms of Fd and +100 to −700 mV for the 3Fe-forms. The working, counter, and reference electrodes were glassy carbon, Pt, and Ag/AgCl, respectively. The temperature dependence of the reduction potentials were measured under the same conditions except that 50 mM HEPES, pH 7.0, was used as the buffer and the temperature was varied between 0 and 80 °C. Temperature was controlled by immersing the electrochemical apparatus in a water bath set at the desired temperature. Potentials were adjusted to the SHE taking into account the temperature dependence of the Ag/AgCl reference electrode (*40*). The isothermal cell arrangement used in this work differs from a nonisothermal setup in that the temperature of both the redox couple under investigation and the reference electrode are varied. However, after correction for the temperature dependence of the reference electrode both systems give identical values for the slope of potential versus temperature, as shown in two independent studies of cytochrome c_{553} from *Desulfovibrio vulgaris* (*32, 41*).

RESULTS AND DISCUSSION

Design of Fd Variants. In all of the mutants investigated in this study, the cluster-coordinating Asp14 residue of the wild-type (WT) 4Fe-Fd (D14) was replaced, either with Asn (D14N), Tyr (D14Y), His (D14H), or Val (D14V). Two additional mutants, where Asp14 was replaced by Ser (D14S) and Cys (D14C), were also examined. Some properties of the latter two proteins were recently reported (*37*). All recombinant proteins contained an iron-sulfur chromophore and could be purified from *E. coli* by following their visible absorption. The yields of all of the recombinant Fds were typically near 0.5 mg/g (wet weight) of *E. coli* cell paste, and these were not significantly affected by the nature of the mutation or the choice of growth medium. It should be noted that in the following, all results with the mutant Fds are compared with those obtained with the recombinant form of the WT Fd.

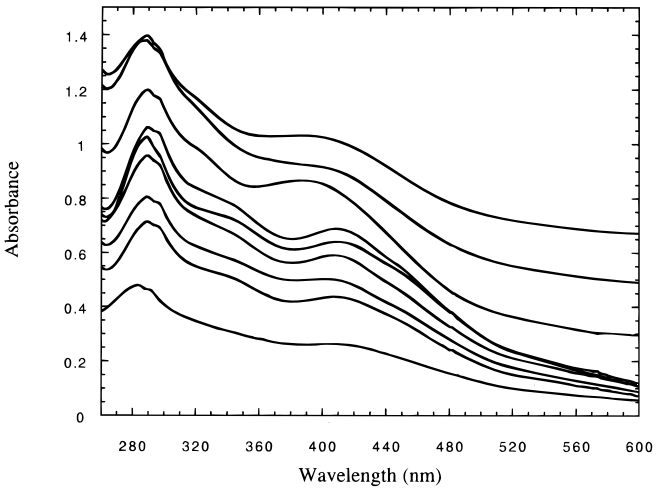

FIGURE 1: UV−visible spectra of oxidized D14X mutants of *P. furiosus* ferredoxin. The Fd variants are, from top to bottom: WT D14/4Fe, D14S/4Fe, and D14C (all of which which have been offset by +0.2 absorbance units), D14N, D14Y, WT D14/3Fe, D14H, D14V, and D14S/3Fe. The samples (25−40 μM) were in 50 mM EPPS buffer, pH 8.0, and the spectra were recorded at 23 °C. The absorbance maxima and ratios for each Fd are summarized in Table 1.

Table 1: Electronic Spectral Characteristics of Variants of *P. furiosus* Ferredoxin

Fd variant	A_{390}/A_{280}	visible maximum	visible maximum/A_{280}	% A_{412} after reduction[a]
WT (4Fe)	0.570	387	0.570	55
D14C (4Fe)	0.731	388	0.714	50
D14S (4Fe)	0.552	390[b]	0.552	65
WT (3Fe)	0.639	408	0.663	63
D14S (3Fe)	0.553	405	0.555	61
D14H (3Fe)	0.660	405	0.665	53
D14N (3Fe)	0.682	409	0.712	67
D14V (3Fe)	0.649	409	0.673	60
D14Y (3Fe)	0.640	405	0.663	65

[a] The samples were reduced at 23 °C with a ∼ 5 molar excess of sodium dithionite. [b] A distinct absorbance maximum was not evident.

UV−Visible Spectroscopy. As shown in Figure 1, the spectral properties of the Fd variants fell qualitatively into two categories, those (D14C and D14S) which were similar to the WT 4Fe-form of protein and those (D14V, D14H, D14Y and D14N) which resembled the WT 3Fe-form (obtained after ferricyanide treatment *in vitro*, ref *11*). The visible absorption maxima and UV/visible absorbance ratios are presented in Table 1. The WT 4Fe- and 3Fe-forms have visible absorbance maxima at 387 and 408 nm, respectively,

which is the expected shift upon such a cluster conversion (*42*). The D14V, D14H, D14Y, and D14N proteins have visible maxima like the 3Fe-form, between 405 and 409 nm, and the ferricyanide-treated D14S mutant also falls into this category. In contrast, the values for the WT 4Fe-form and the D14S and D14C mutants are 387−390 nm. The A_{390}/A_{280} ratios for all of these 3Fe proteins were also very similar, although not identical, see Table 1. These data indicate that the D14V, D14H, D14Y, and D14N mutants, together with the ferricyanide-treated D14S mutant (see Table 1), all contain a [3Fe-4S] cluster, and this is substantiated by their redox properties described below. Such a conclusion has also been confirmed by detailed EPR, MCD, and resonance Raman analyses.[2,3] In contrast, the visible absorption data suggest that D14C and D14S mutants contain a [4Fe-4S] cluster, and this has also been demonstrated by EPR and NMR spectroscopic analyses (*37*, *43*).

Figure 1 also indicates that the precise electronic spectrum observed from the Fd variants is dependent on the nature of the residue at position 14, regardless of cluster type. Hence, the spectra of the various 4Fe-forms are not superimposable. The gain of an Fe-S charge-transfer band in the D14C mutant compared to the WT D14 protein explains the increase in the UV/visible ratio (see also ref *42*), but even the D14S and WT D14 proteins are distinguishable, in particular, the former does not exhibit a distinct visible absorption maximum. The same is true of the various 3Fe-forms, although in this case, where the mutated residue cannot be directly coordinating an Fe atom, the results are harder to rationalize. For example, their visible maxima/A_{280} ratios are all very similar (0.66 ± 0.01, see Table 1), except for the D14N protein where the ratio is 0.71 and the 3Fe-form of the D14S protein which has a lower ratio (0.555). Significant differences between all the 3Fe-forms are also manifest in the near-UV region (Figure 1). The addition of an extra Tyr to the protein (D14Y) did not significantly alter the UV/visible absorbance ratio, even though free tyrosine has significant absorption in the UV region (1340 $M^{-1}cm^{-1}$ at 274 nm, ref *44*). The reason for this remains unclear.

Fds typically undergo an approximate 50% decrease in their visible absorption upon complete reduction of their 4Fe-cluster. Since the assay for the biological activity of the mutant Pf Fds was dependent upon changes in their visible absorption upon reduction, this phenomenon was characterized for each protein. As shown in Table 1, the extent of the change in the extinction coefficient upon reduction with excess sodium dithionite (which is assumed to be complete, see below) is apparently independent of whether the Fd is a 3Fe- or 4Fe-form. The Fd variants lost between 50% (D14C) and 33% (D14N) of their visible absorption (measured at 412 nm, see Table 1). Due to the high absorbance of dithionite in the UV region, UV/visible ratios could not be calculated, but clearly the visible absorption spectra of the various Fd mutants, both 3Fe- and 4Fe-forms, are affected by the nature of the residue at position 14.

[2] Staples, C. R., Duderstadt, R. E., Fu, W., Zhou, Z. H., Brereton, P., Verhagen, M. F. J. M., Adams, M. W. W., and Johnson, M. K., submitted for publication.

[3] Duderstadt, R. E., Staples, C. R., Fu, W., Zhou, Z. H., Brereton, P., Verhagen, M. F. J. M., Adams, M. W. W., and Johnson, M. K., unpublished data.

Table 2: Reduction Potentials of Variants of *P. furiosus* Ferredoxin

Fd variant	E_m[a] (mV)	$-\Delta E_m/\Delta$pH (mV)	pK (pK_{ox}, pK_{red})	$E_{m,alk}$[b] (mV)
WT (4Fe)	−368 (−379)	−1.6		
D14C (4Fe)	−426 (−421)	−4.4		
D14S (4Fe)	−501 (−495)	−57[c]	4.7	−501
WT (3Fe)	−203 (−208)	−44[d]	4.2, 5.9	−219
D14H (3Fe)	−129 (−131)	−28[d]	4.7, 5.9	−130
D14N (3Fe)	−125 (−127)	−30[c]	3.3	−130
D14V (3Fe)	−188 (−190)	−54[c]	4.5	−192
D14Y (3Fe)	−148 (−157)	−44[c]	3.8	−162
D14S (3Fe)	−85 (ND[e])	ND		

[a] Determined at pH 7.0, 23 °C. The values in parentheses are derived from the best fit to the temperature-dependent data (see Figure 4). [b] Determined at pH 10.0, 23 °C. [c] The values were calculated using the reduction potentials measured at pH 3 and 3.5. [d] The values were calculated using the reduction potentials measured at pH 4.5 and 5.5. [e] Not determined

Electrochemistry. The reduction potentials of the Fd variants were determined by direct electrochemistry, and the results are summarized in Table 2. As previously noted (*34*), the value for the recombinant Fd is the same as that determined for the native Fd as purified from Pf. The reduction potential of the recombinant 3Fe form of Pf Fd was similar to that (−190 mV) obtained previously (*45*). For reasons that are not clear, the potentials of both the 3Fe- and 4Fe-forms of the protein determined by electrochemical techniques (cyclic voltammetry or differential pulse) are 30−40 mV more negative than those generated by bulk redox titrations monitored by EPR spectroscopy (*28*). The values measured herein for the Fd variants (at pH 7) fall into two groups in accordance with the cluster type, with the 3Fe-forms (D14N, D14V, D14Y, and D14H) being more than 150 mV more positive than the 4Fe-forms (D14, D14C, and D14S). Interestingly, all of the mutant 3Fe-forms had reduction potentials more positive (up to almost 120 mV) than that of the WT D14 3Fe-protein (see below). The reduction potentials of the 4Fe-forms, where D14 > D14C > D14S, is readily explained by the pK_a value of residue 14, where Asp (4.0) < Cys (8.5) < Ser (16) (assuming that each is a cluster ligand, see below). Thus, compared to Cys, Asp is a better electron withdrawing group and stabilizes the reduced cluster, while Ser is a stronger electron donor and stabilizes the oxidized form. The reduction potentials of the various 3Fe forms cannot be explained in this manner as they (obviously) do not bind a cluster Fe atom and no correlation is found by a similar electrochemical analysis.

The pH dependence of the reduction potentials of all Pf Fd variants were determined over the range pH 3.0−10 and the results are summarized in Table 2. Only the WT 4Fe-form (Figure 2a), the D14C mutant (Figure 2a), and the 3Fe-form of the D14S mutant (Figure 2b) showed no dramatic change over this pH range. Nevertheless, for the WT 4Fe-form and the D14C mutant, the changes were linear and reproducible, with values of −1.6 and −4.4 mV/pH unit, respectively. The only other Fds that have been examined in this regard are the multicluster proteins from *Azotobacter vinelandii* (Av), which contains one 3Fe- and one 4Fe-cluster (*46*) and from *Clostridium pasteurianum* (Cp), which has two 4Fe-centers. In these cases, the pH dependence of their [4Fe-4S] centers was larger (∼ −16 mV/pH unit for Av Fd and between −11 and −16 mV/pH unit for Cp Fd (*47*−*49*) than those seen for the Pf Fd proteins, although less than

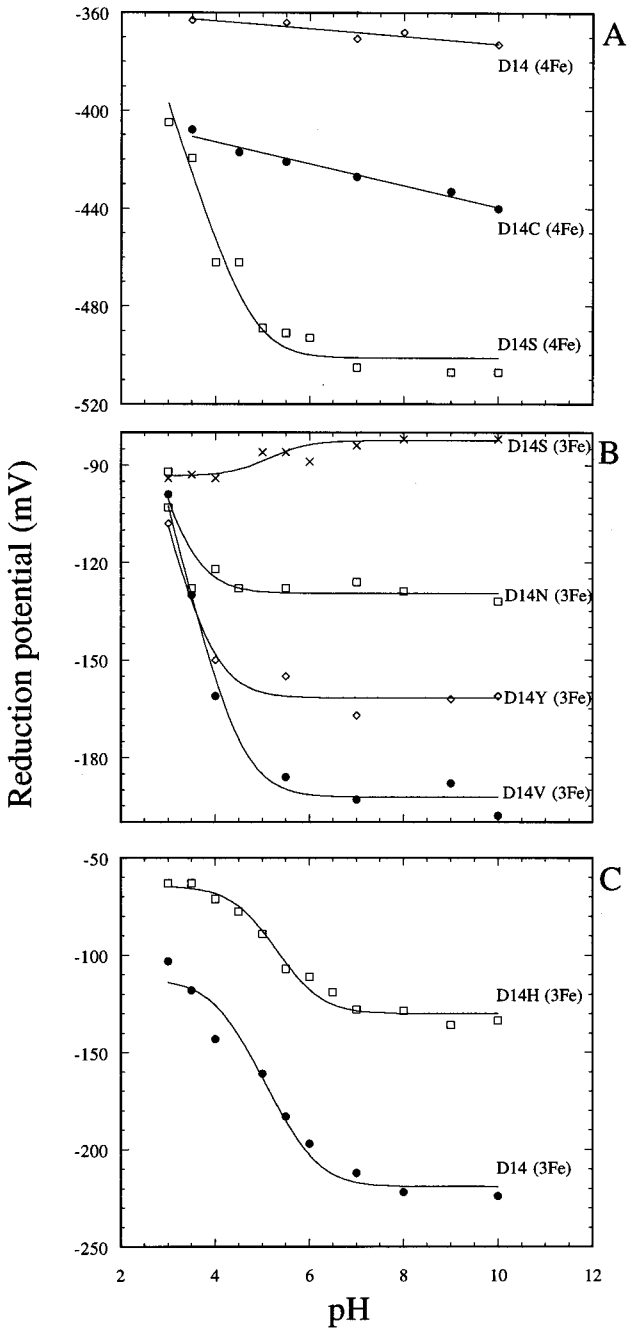

FIGURE 2: (A) The pH dependence of the reduction potentials for the 4Fe-forms of *P. furiosus* ferredoxin. The values for the WT (D14) and two mutant forms (D14S and D14C) were obtained at 23 °C as described in Materials and Methods. All potentials are relative to the SHE. (b) The pH dependence of the reduction potentials for the 3Fe-forms of *P. furiosus* ferredoxin. The values were obtained at 23 °C as described in Materials and Methods. The indicated samples represent the D14N, D14V, and D14Y mutants, together with the 3Fe-form of the D14S mutant obtained by ferricyanide treatment. All potentials are relative to the SHE. (c) The pH dependence of the reduction potentials for the 3Fe-forms of the WT (D14) and D14H mutant of *P. furiosus* ferredoxin. The values were obtained at 23 °C as described in Materials and Methods. All potentials are relative to the SHE.

that attributable to an ionizable group (−58.1 mV/pH unit at 20 °C, ref *50*). To investigate possible causes of the pH effect, the temperature dependence of the midpoint potential of the D14C mutant of Pf Fd was determined at pH 4.0, 7.0, and 10.0 over the range 0−80 °C. While the values decreased linearly with increasing temperature (see below), the temperature response was independent of pH (data not shown). Thus, in the case of the D14C mutant, at least, the small but significant pH effect appears to be a result of minor perturbation of the electrostatic and/or H-bonding interactions around the cluster.

In contrast to the other 4Fe-forms of Pf Fd, the reduction potential of the D14S (4Fe) mutant showed a marked pH dependence in the acidic range, see Figure 2a. That Ser14 plays a direct role in this pH response is strongly suggested by the absence of a similar pH effect in the WT protein and the D14C mutant. Moreover, a recent NMR study of the D14S mutant showed that Ser14 is a ligand to the cluster at pH 7 (*43*). Hence, the pH response can be analyzed by assuming that electron transfer is coupled to the addition of a proton to the coordinating serinate (L^-, eqs 1 and 2), which is a stronger acid when coordinated to the oxidized form of the cluster than it is when coordinated to the reduced form. Note that upon protonation, it is not clear if serine remains a cluster ligand or is replaced by water/hydroxide or even another protein side chain. In any event, the redox behavior of such a system is described by a modified form of the Nernst equation (eq 3), where $E_{m,obs}$ is the observed reduction potential, K_H is the acid dissociation constant, $E_{m,alk}$ is the reduction potential under alkaline conditions (pH ≫ p*K*), and other terms have their usual meanings. The slope of the fit (eq 3) between pH 3 and 4 was −55 mV/pH unit at 23 °C (see Figure 2a), in excellent agreement with theory (*50*), and the calculated p*K* (of H^+ addition) was 4.75 ± 0.13. These data indicate that equilibrium (eq 2) is established in the time of the voltammetric scan (*46*).

$$[\text{4Fe-4S}]^{2+}\cdot L^- + e^- = [\text{4Fe-4S}]^{1+}\cdot L^- \qquad (E_{m,alk}) \quad (1)$$

$$[\text{4Fe-4S}]^{1+}\cdot L^- + H^+ = [\text{4Fe-4S}]^{1+}\cdot LH \qquad (1/K_H) \quad (2)$$

$$E_{m,obs} = E_{m,alk} + \{(2.303RT/F)\log\{1 + [H^+]/K_H\} \quad (3)$$

The reduction potentials of the 3Fe-forms of Pf Fd were also determined over the pH range 3−10, and all of them (except the D14S mutant) showed a pH response, see Figures 2b and 2c. For two of the proteins, the D14H mutant and the WT 3Fe-form, the data were fitted with two p*K*s according to eq 4. The pK_{ox} and pK_{red} values were 4.7 and 5.9,

$$E_{m,obs} = E_{m,alk} + (2.303RT/F) \log\{K_{red} + [H^+]/K_{red}\cdot K_{ox} + K_{red}\cdot[H^+]\} \quad (4)$$

respectively, for the D14H mutant and 4.2 and 5.9 for the WT form. The other three 3Fe-forms, D14N, D14V, and D14Y, also showed an increase in potential at low pH, see Figure 2b. However, in these cases the responses were similar, and the data could be fitted with just one p*K* as described in eq 3 with calculated p*K* values of 3.3, 4.5, and 3.8, respectively. Prior spectroscopic studies have shown that reduced [3Fe-4S] centers can exist in two pH-dependent forms (*51*, *52*), and a pH effect reflecting a single protonation site was observed for the reduction potential of the [3Fe-4S] cluster in Av Fd (p*K* 7.8; refs *46*, *53*). Why the p*K* of the 3Fe-cluster in Av Fd should be so much higher than that in Pf Fd, see Table 2, is not clear at present. It seems reasonable to suggest that this pH effect is due to protonation

of the cluster itself, presumably at an inorganic sulfur atom, and that this effect is not dramatically perturbed by the amino acid side chain (position 14 in Pf Fd) that would normally interact with the fourth Fe site, if present. With Pf Fd, the ionizable side chains of the Asp14 (WT) or His14 variants must influence the properties of the cluster directly as these exhibit a second p*K*. From Table 2, the p*K* of the 3Fe-cluster in Pf Fd varies from 3.3 to 4.5 (with Asn, Val, or Tyr at position 14), suggesting that the second p*K* values from the ionizable residues (Asp, His) are near 5.9. In their protonated forms they would not be expected to have a significant influence on the p*K* of the cluster (4.2−4.7). Consequently, at low pH (∼ 3) the reduction potentials of all 3Fe-forms converge near −100 mV, see Figures 2b and 2c. That of the D14H variant is slightly higher (−65 mV), which might be expected as of all variants only this one would have a positively charged residue in the position 14 pocket.

The one exception to the general pH-dependent response of the 3Fe-forms of Pf Fd is the D14S mutant. As shown in Figure 2b, its reduction potential was almost linear over the pH range 3 to 10, and decreased slightly (approximately 10 mV) at low pH, thus reversing the trend seen for the other 3Fe-proteins. Why Ser at position 14 should prevent the putative cluster protonation reaction is not clear at present. In any event, at neutral pH and above, the D14S 3Fe-form had the most positive midpoint potential of all the 3Fe-forms examined (note the 4Fe-form of this protein had the most negative reduction potential, see Table 2). The other 3Fe-forms under similar conditions (pH ≥ 7) exhibited a range of reduction potentials (−203 to −125 mV), but how to correlate the values with the residue at position 14 is not obvious (some attempts to do this from a thermodynamic perspective are addressed below). On the other hand, the protonation event at low pH disrupts to a large extent the influence residue 14 has on the reduction properties of the cluster. The absence of this pH response in the D14S mutant suggests that the p*K* for cluster protonation in this protein is below 3.0. This is supported by the great similarity in the VTMCD spectra of the D14S protein and the other D14 mutants (at pH 7) indicating the same protonation states for their clusters.[3] Thus, the identity of the residue at position 14 in Pf Fd not only determines the type of cluster that can be accommodated by the protein (3 or 4Fe), but also clearly can have a dramatic influence on the redox chemistry of that cluster, even by potentially innocuous residues such as Val, Tyr, and Asn.

Temperature Dependence. Before investigating the temperature-dependent redox and kinetic properties of the various mutants, their thermal stability was assessed. As mentioned, the 4Fe-form of WT Pf Fd shows no denaturation (as monitored by visible absorption at pH 7.0) after 12 h at 95 °C (*28*). The 4Fe-forms of the D14C and D14S mutants and the 3Fe-forms of the WT and D14S, D14N, D14V, D14Y, and D14H mutants, were also unaffected by the same treatment. To determine if any differences in the stability of the variants and WT protein could be detected, the proteins were examined under various pH conditions. Remarkably, at pH 2.5, the WT protein showed a decrease in visible absorption on a reasonable time scale (minutes) at 80 °C. At low pH it is assumed that the stability is maintained by nonionic interactions, since acidic groups should be protonated. At pH 2.5, the WT 4Fe-protein had a half-life ($t_{1/2}$)

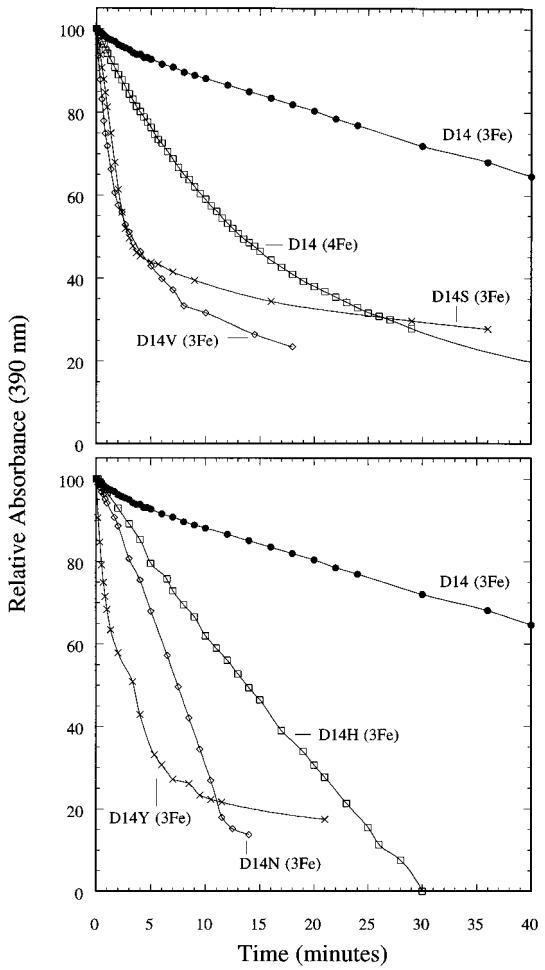

FIGURE 3: The thermal stability of the variants of *P. furiosus* ferredoxin. The indicated protein (approximately 0.11 mg/mL in 50 mM glycine/HCl, pH 2.5) was incubated at 80 °C, and denaturation was assessed by measuring the loss of absorption at 390 nm.

of ∼15 min at 80 °C, although, as shown in Figure 3, denaturation did not follow first-order kinetics. Surprisingly, the 3Fe-WT protein was more stable, with a $t_{1/2}$ value of about 1 h. Moreover, at pH 2.5 and 80 °C, the 3Fe-variants exhibited a range of stabilities, and a variety of distinctive denaturation curves were obtained indicating nonideal behavior, e.g., with D14H, see Figure 3. Further analyses of the kinetics will not be presented here, but clearly, residue 14 can have a large effect on the overall stability of the Fd molecule, although not enough of one to preclude the following temperature-dependent analyses.

The reduction potentials of all of the Pf Fd variants, both 3Fe- and 4Fe-forms, were examined within the temperature range 0−80 °C, see Figure 4. The data presented here for the WT protein up to 90 °C, obtained by direct electrochemistry, are in good agreement (see thermodynamic values given below) with those previously reported for the native Fd purified from Pf, which were determined by bulk electrochemical titrations monitored by EPR spectroscopy (*54*). However, the transition seen at 80 °C in the latter study was not evident by the direct method, see Figure 4. The temperature-dependent behavior of the reduction potential of native Fd from Pf, determined by cyclic voltammetry, was virtually identical to that of the recombinant WT protein (data not shown) and an 80 °C transition was not observed. We

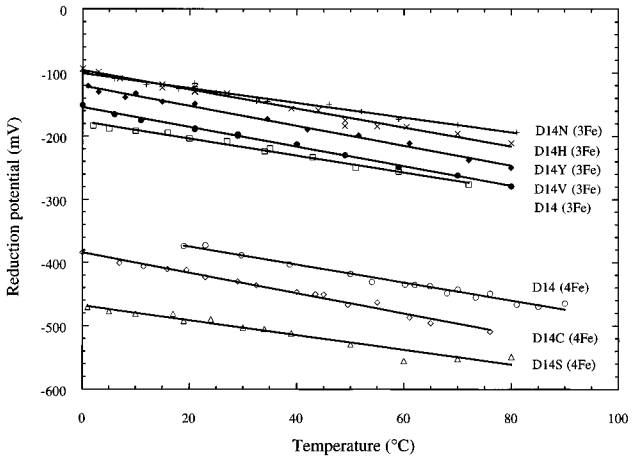

FIGURE 4: Temperature dependence of the reduction potentials of variants of *P. furiosus* ferredoxin. The values were obtained at pH 7.0 as described in Materials and Methods. All values are relative to the SHE.

Table 3: Summary of the Thermodynamic Parameters of Variants of *P. furiosus* Ferredoxin

D14X	E_m[a] mV	ΔmV/K	$\Delta G^{\circ\prime}$ kJ mol^{-1}	$\Delta S^{\circ\prime}$ kJ mol^{-1} K^{-1}	$\Delta H^{\circ\prime}$ kJ mol^{-1}	$T\Delta S^{\circ\prime}$ kJ mol^{-1}
WT (4Fe)	−368	−1.43	35.5	−203	−24.6	−60.1
D14C (4Fe)	−426	−1.61	41.1	−221	−24.2	−65.3
D14S (4Fe)	−501	−1.16	48.3	−177	−4.2	−52.5
WT (3 Fe)	−203	−1.34	19.6	−195	−38.0	−57.6
D14H (3Fe)	−129	−1.50	12.5	−210	−49.7	−62.2
D14N (3Fe)	−125	−1.16	12.1	−177	−40.4	−52.5
D14V (3Fe)	−188	−1.55	18.1	−215	−45.5	−63.6
D14Y (3Fe)	−148	−1.58	14.3	−218	−50.2	−64.5
D14S (3Fe)	−85	ND[b]	ND	ND	ND	ND

[a] At pH 7, 23 °C, and given relative to the SHE. [b] Not determined.

therefore conclude that this transition is peculiar to the EPR-monitored bulk method, perhaps arising as an artifact of freezing which is necessary for spectroscopic analysis. In fact, by the direct method, none of the Fd variants exhibited a transition, and in all cases, their reduction potentials decreased by between 1.16 and 1.61 mV/°C with increasing temperature, independent of whether the protein contained a 3Fe- or 4Fe-center, see Table 3. These data are in contrast to those obtained with the Fd of the mesophile, *D. vulgaris* (Dv), the only other Fd which has been studied in this regard. The reduction potential of the Dv protein, which contains a [4Fe-4S] cluster, changed by −0.40 ± 0.1 mV/°C over the range 8−46 °C (*30*). A series of [4Fe-4S] containing Hipips exhibited temperature-dependent redox potentials in the range −1.13 mV/°C to −2.39 mV/°C (*6*).

Thermodynamic Parameters. In the isothermal system used here for Pf Fd, the slope ($\delta E_m/\delta T$) of a plot of reduction potential versus temperature, see Figure 4, is related to the thermodynamic entropy parameter $\Delta S^{\circ\prime}$ by eqs 5 and 6. The relevant data for the Fd variants are summarized in Table 3.

$$\Delta S^{\circ\prime}_{rc} = nF(\delta E^{\circ\prime}/\delta T)_p \quad (5)$$

$$\Delta S^{\circ\prime} = \Delta S^{\circ\prime}_{rc} - 65.2 \quad (6)$$

The $\Delta S^{\circ\prime}$ value for the recombinant WT protein determined in this study (−203 J mol^{-1} K^{-1}) is in agreement with that previously reported for the Fd purified from Pf (−210 J mol^{-1} K^{-1}; ref *45*). For the different variants of Pf Fd, however, the magnitude of the $\Delta S^{\circ\prime}$ values are independent of the cluster type and of the cluster reduction potential, see Figure 5. It should be noted that the overall entropy change for a redox reaction involving a given protein is equal to the difference in the specific entropy in each redox state, as shown in eq 7 (*29*).

$$\Delta S^{\circ\prime}_{rc} = S^{\circ\prime}_{red} - S^{\circ\prime}_{ox} \quad (7)$$

Thus, $\Delta S^{\circ\prime}_{rc}$ values are not directly comparable to other properties obtained with a specific redox state of the protein, e.g, data presented in Figure 3, since the specific entropy of a given redox state is unknown. Nevertheless, for the same type of cofactor, such as a cubane cluster, the magnitudes of the $\Delta S^{\circ\prime}$ values for different proteins might give insights into the cofactor environment in its different redox states. For example, for six Hipips obtained from different mesophilic photosynthetic bacteria, the $\Delta S^{\circ\prime}$ values ranged from −230 to −109 J mol^{-1} K^{-1} (a range of 121 J mol^{-1} K^{-1}, ref *6*). For the same Hipip proteins, Soriano et al. (*31*) reported more negative values (−340.7 to −170 J mol^{-1} K^{-1}) than those determined by Heering et al. (*6*), a discrepancy ascribed to the different solution conditions used in obtaining the measurements. In any event, the values for the Pf Fd mutants of −221 to −177 J mol^{-1} K^{-1} (a range 44 J mol^{-1} K^{-1}) are in the same range as those obtained for the Hipip proteins, although they are more negative than that (−103 J mol^{-1} K^{-1}) for DvFd. In considering other types of redox cofactor, the values for Pf Fd are within the range reported for the rubredoxin of Pf (−251.2 J mol^{-1} K^{-1}, ref *45*), but are significantly more negative than the values reported for various heme proteins including cytochrome *c* (−120 J mol^{-1} K^{-1}) and hemoglobin (−157 J mol^{-1} K^{-1}), and also for the Rieske [2Fe-2S]-containing protein of the bc_1 complex (−155 J mol^{-1} K^{-1}, refs *17*, *29*, *32*). Whether there is a relationship between the large negative entropy values for redox proteins containing [4Fe-4S] (or 1Fe) centers, and particularly with those involving the presumably more rigid hyperthermostable proteins of Pf, and protein stability remains to be established.

Although the $\Delta S^{\circ\prime}$ values for the variants of Pf Fd are independent of cluster type and cluster potential, see Figure 5, the electronic spectra of Fd proteins were examined to determine if any correlation existed between reduction potential and cluster environment. The visible maxima reflect the polarity of the cluster environment, and variations in reduction potential might indicate changes in the amount of cluster solvation (*55*, *56*). This in turn might ultimately be related to the independent components of the entropy of the system (see, for example, ref *32*). For example, the effect of DMSO/water mixtures on the visible absorbance maxima of the Cp Fd and of synthetic [4Fe-4S] analogs (*57*) indicated a correlation between DMSO concentration, reduction potential, and visible maxima. The latter were red-shifted by 13.7 mV/nm for the Fd and by 6−10 mV/nm for the analogs

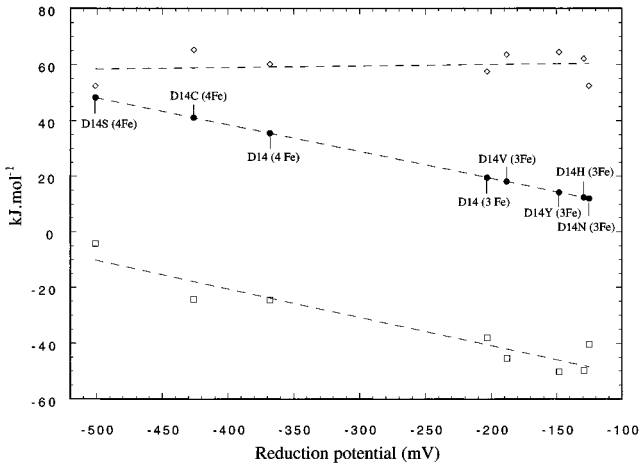

FIGURE 5: Thermodynamic parameters derived from the temperature-dependent midpoint potentials of the variants of *P. furiosus* ferredoxin. The calculated $\Delta G^{\circ\prime}$ (solid circles), $-T\Delta S^{\circ\prime}$ (tilted open squares), and $\Delta H^{\circ\prime}$ (open squares) values for the various proteins are depicted. Reduction potentials were calculated as described in Materials and Methods. The thermodynamic parameters $\Delta G^{\circ\prime}$, $\Delta S^{\circ\prime}$, and $\Delta H^{\circ\prime}$ were derived from eqs 5, 6, 8, and 9. The relevant parameters are summarized in Table 3.

as the cluster environment became more hydrophobic with increasing DMSO concentrations. Similarly, for a variety of Hipips, a linear correlation of 19.8 mV/nm was found between the position of the absorbance band near 385 nm and reduction potential (*6*). However, although the Pf Fd variants show small differences in their absorption maxima, particularly for the 3Fe-forms (Table 1), there was no correlation between absorbance maximum and reduction potential for these proteins (data not shown). In addition, no relationship was found between any of the latter indices and the hydrophobicity of the residue at position 14, a parameter which should also reflect solvent accessibility to the cluster. Hence, we conclude that the changes in the reduction potential of the various forms of Pf Fd do *not* arise from significant changes in protein rigidity or cluster solvation. The significance of this conclusion and how it is related to the variation in the $\Delta S^{\circ\prime}$ values shown in Figure 5 also remain to be determined.

Enthalpy. The change in the Gibbs free energy term ($\Delta G^{\circ\prime}$) was calculated from the measured reduction potentials (eq 8). The enthalpy term $\Delta H^{\circ\prime}$ was then derived using the Gibbs−Helmholtz equation (eq 9) where the temperature was 296 K. A summary of the results and

$$\Delta G^{\circ\prime} = -nFE^{\circ\prime} \quad (8)$$

$$\Delta H^{\circ\prime} = \Delta G^{\circ\prime} + T\Delta S^{\circ\prime} \quad (9)$$

the calculated thermodynamic parameters is presented in Table 3. Again, the $\Delta H^{\circ\prime}$ value for the WT recombinant form (−24.6 kJ mol^{-1}) is similar to that reported for the protein purified from Pf (−20.9 kJ mol^{-1}, ref *45*). For the Fd variants, a linear correlation between $\Delta H^{\circ\prime}$ and redox potential was observed with a slope (−102 kJ mol^{-1}) similar to that of the $\Delta G^{\circ\prime}$ plot (which is by definition −96.5 kJ mol^{-1}). These results suggest that it is the enthalpy term that is a major determinant of redox potential. The range of values that were obtained span ∼46 kJ mol^{-1}, which is similar to that reported for various Hipips (50.3 kJ mol^{-1}, ref *6*), although with Pf Fd the range is much smaller for a given cluster type (20.4 kJ mol^{-1} for the 4Fe-forms, 12.2 kJ mol^{-1} for the 3Fe-forms). This might be expected as the Hipips were obtained from different bacteria, whereas the Fds differ by only one amino acid. However, for reasons which are not clear, the actual values obtained for the Pf proteins are about half those obtained for the different Hipips (−49 to −99 kJ mol^{-1}, from data obtained over a 20 °C range).

A better comparison with the Pf Fd data is provided by a study of nine single amino acid mutants made at three different (noncluster coordinating) positions of Cv Hipip (*31*). The variation in the $\Delta H^{\circ\prime}$ values (approximately 30 kJ mol^{-1}) is similar to that seen for the Pf proteins. It was concluded from the Hipip variants that although aromatic residues have close interactions with the [4Fe-4S] cluster, their nonconservative mutation had little effect on the thermodynamic parameters ($\Delta H^{\circ\prime}$ and $\Delta S^{\circ\prime}$) and therefore are relatively unimportant in defining the cluster redox potential, particularly when compared to the effect of the number and orientation of peptide amide groups near the cluster (*10*). In another study (*33*), it was found that the C77S mutation (where Cys77 is a cluster ligand) caused a 53.6 kJ mol^{-1} increase in the $\Delta H^{\circ\prime}$ value and a 169 J mol^{-1} K^{-1} increase in the $\Delta S^{\circ\prime}$ value (compared to the WT Cv Hipip), changes that are much greater than those observed with the Pf Fd variants. However, there was only a modest change in the reduction potential of the C77S mutant (−30 mV). Such an effect is consistent with an isoequilibrium relationship, whereby a more favorable entropy value (more positive) is compensated for by a less favorable (more positive) enthalpy term (*58*). Although it is difficult to speculate on a similar trend in the Pf Fd variants examined here because of the small overall changes in the parameters, the corresponding values for the various Fds (except the D14N mutant) do offset each other to some degree, see Figure 5. Dv 4Fe-Fd is the only other Fd for which thermodynamic data are available (*30*), but this gave a positive enthalpy value (9.65 kJ mol^{-1}), in contrast to variants of Pf Fd (Table 3) and Cv Hipip (*6*).

Biological Activity. The ability of the Pf Fd variants to function as electron carriers for two oxidoreductases from Pf was investigated using both direct and coupled assay systems. The direct assay used pyruvate ferredoxin oxidoreductase (POR, ref *20*), which reduces Fd according to eq 10. The coupled assay involved POR and ferredoxin: NADP oxidoreductase (FNOR, ref *26*). FNOR accepts electrons from reduced Fd and reduces NADP, eq 11. Hence with a combination of POR, FNOR, and Fd, pyruvate oxidation can be coupled to NADP reduction.

$$\text{Pyruvate} + \text{CoASH} + 2\text{Fd}_{ox} \rightarrow \text{Acetyl-CoA} + \text{CO}_2 + \text{H}^+ + 2\text{Fd}_{red} \quad (10)$$

$$2\text{Fd}_{red} + \text{H}^+ + \text{NADP} \rightarrow \text{NADPH} + 2\text{Fd}_{ox} \quad (11)$$

The ability of Pf POR to reduce the D14C and D14S mutants has been previously reported (*37*), and the results are discussed below. However, preliminary analyses with WT Fd showed that the POR specific activity decreased as the POR concentration in the assay medium increased. As shown in Figure 6, this effect was independent of the electron carrier used (WT 4Fe-form or methyl viologen) and was also

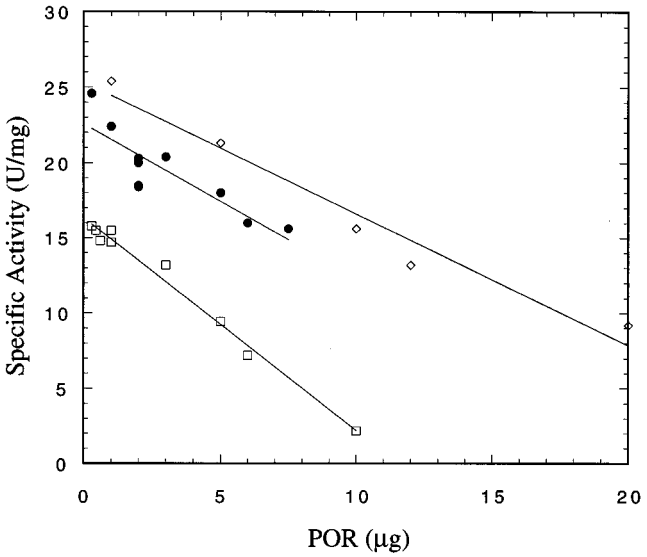

FIGURE 6: Effect of POR concentration on its specific activity. The assays were performed as described in Materials and Methods. The electron carriers were WT 4Fe-Fd (open squares, 50 μM), methyl viologen (solid circles, 1 mM), and WT 4Fe-Fd (tilted open squares, 25 μM), measured by following the reduction of metronidazole (100 μM).

Table 4: Kinetic Parameters for the Wild-Type and Mutant Forms of *P. furiosus* Ferredoxin

		POR[a]		POR/SuDH[a]	
Fd variant	E_m[b] (mV)	K_m (μM)	V_m (units/mg)[c]	K_m (μM)	V_m (units/mg)[d]
WT (4Fe)	−454	22 (7)	25 (2)	1.7 (0.3)	5.5 (0.3)
D14C (4Fe)	−503	11 (4)[e]	8.4 (1)[e]	0.2 (0.05)	6.4 (0.3)
D14S (4Fe)	−558	16 (13)	10 (2)	0.5 (0.1)	6.8 (0.3)
WT (3Fe)	−279	50 (12)	46 (4)	1.7 (0.5)	4.2 (0.3)
D14S (3Fe)	−148	50 (20)	47 (9)	NA[f]	<0.5
D14H (3Fe)	−214	39 (15)	33 (5)	NA[f]	<0.5
D14N (3Fe)	−191	23 (4)	20 (1)	NA[f]	<0.5
D14V (3Fe)	−276	40 (7)	37 (3)	7.7 (4)	3.9 (1.0)
D14Y (3Fe)	−238	31 (10)	39 (4)	NA[f]	<0.5

[a] Kinetic parameters for the indicated forms of Fd in the POR and the coupled POR/FNOR systems were measured at 80 °C and pH 8.0 as described in Materials and Methods. Standard deviations are given in parentheses. [b] Reduction potential determined at pH 7.0, 80 °C vs SHE. [c] One unit/mg is the reduction of two μmols of Fd per min/mg of POR. [d] One unit/mg is the reduction of two μmols of Fd per min/mg of FNOR. [e] Taken from ref *37*. The specific activity was corrected for the POR concentration (see text for discussion). [f] K_m value could not be determined because of the low activity.

observed when the concentration of Fd (WT 4Fe-form) was kept constant using a metronidazole-linked assay (*37*). In addition, a 2-fold increase in the concentrations of pyruvate, coenzyme A, and Mg^{2+} (using 50 μM WT 4Fe-Fd) did not increase the specific activity of POR. Therefore, the concentration-dependent effect appears to be a property of the enzyme itself. While this is very unusual, and may perhaps provide insight into its catalytic mechanism, the following results were obtained using a constant POR concentration, and a conversion factor (see Figure 6) has been used to compare them with specific activities previously reported with this enzyme (*20*, *37*, *45*).

Pf POR reduced all of the Fd variants under study, both 4Fe- and 3Fe-versions, and the kinetic parameters are given in Table 4. The results with the WT and D14S 4Fe-forms and with the WT 3Fe-forms were in reasonable agreement

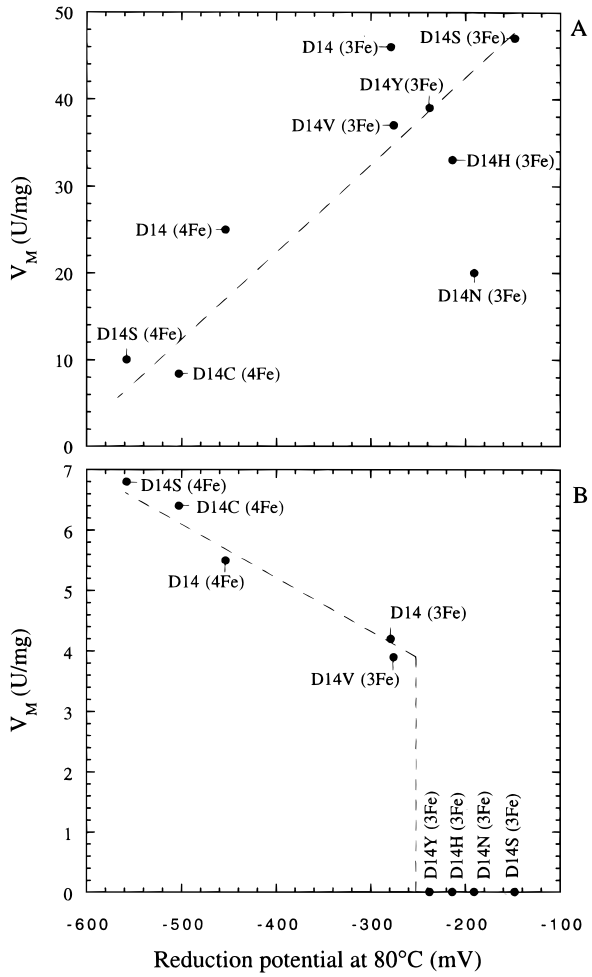

FIGURE 7: (A) Effect of reduction potential of variants of *P. furiosus* ferredoxin on the activity of pyruvate ferredoxin oxidoreductase at 80 °C. Reduction potentials are taken from Figure 4 with the exception of the 3Fe-form of the D14S mutant. This was estimated to be −148 mV from the value measured at 23 °C (see Table 2) assuming Δ mV/K = −1.16 (as determined for the 4Fe-form). The V_m values were taken from Table 4. (B) Effect of reduction potential of variants of *P. furiousus* ferredoxin on the activity of ferredoxin: NADP oxidoreductase at 80 °C. Reduction potentials were taken from Figure 4, and the V_m values were taken from Table 4.

with those obtained previously (*37*), after correcting, in the case of the V_m values, for the amount of POR used in the assays. In particular, the mutant 4Fe-forms (D14C and D14S) exhibited decreased V_m values compared to the WT protein, suggesting that the lower midpoint potentials of these mutants affect their capacity to efficiently accept electrons from POR. This is supported by the V_m values for the various 3Fe-forms. POR has a similar apparent affinity for all of them, with K_m values in the range 37 ± 14 μM, but, as indicated in Figure 7a by the dotted line, there is a general increase in activity with increasing reduction potential (measured at 80 °C) of the Fd. The notable exception is the D14N (3Fe) mutant which is about 2-fold less active than the other 3Fe-forms, although it is twice as active as the D14S 4Fe-form, which had the lowest specific activity as well as the lowest reduction potential. At the other extreme was the D14S 3Fe-form, with the most positive potential and the highest V_m value. Thus, the reduction potential of the Fd, rather than cluster type or the nature of the residue at position 14, appears to be the predominant factor in determining efficiency of reduction by POR. The

anomalous results with the D14N mutant are hard to rationalize and are not reflected in any of its other properties discussed above.

A more informative view of the biological function of a redox protein is provided by a coupled assay in which electron transfer (rather than just reduction or oxidation) is measured. This also lessens the effects that may be caused by nonspecific interactions (*59*). The POR/FNOR coupled assay was designed to specifically measure the interaction of the Fd with FNOR, wherein an excess of POR ensured that the rate limiting step was not the reduction of Fd by POR. Hence, under the standard assay conditions (see Materials and Methods), the rate of the reaction (measured by NADP reduction) was unaffected by a 2-fold increase in POR concentration, but did increase with increasing concentrations of FNOR. It was also empirically determined that the rate of oxidation of Fd by FNOR was slower than the reduction of Fd by POR. For example, the rate of reduction of the WT 4Fe-form by POR was 14-fold higher than Fd oxidation by FNOR. It should be noted that oxidized WT Fd is a poor substrate in the NADPH-dependent reaction catalyzed by FNOR (the reverse of eq 11, ref *26*). The WT, D14C, and D14S did not support significant rates of NADPH oxidation. Moreover, although the reduction potential of NADPH (E_m −320 mV, pH 7.0, 25 °C) is more negative than that of any of the 3Fe-forms (Table 2), only very low rates of NADPH oxidation were observed and they were independent of the 3Fe-form used (0.060 ± 0.015 μmol of NADPH oxidized per minute/mg of FNOR). These data serve to emphasize the utility of the coupled assay system.

As shown in Table 4, the three 4Fe-forms (WT, D14S, and D14C) were all active in the coupled assay, but of the 3Fe-forms, only the WT and D14V mutant supported NADP reduction. The apparent K_m values for the five active Fds were all very low (<8 μM, see Table 4), with that for the D14C 4Fe-mutant being almost an order of magnitude lower than that for the WT 4Fe-protein. The reason for this is not clear at present, but the V_m values with the three 4Fe-forms were similar (6.2 ± 0.7 units/mg) indicating that position 14, while affecting the apparent affinity of the Fd for FNOR, does not influence the rate of electron transfer to the enzyme. The rates of intermolecular electron self-exchange for these three 4Fe-forms of the Fd have been determined by NMR and they follow the trend D14C > D14S > WT (*60*). It was suggested (*60*) that residue 14 plays a role in "gating" electron transfer to/from the cluster, but this appears not to be the case with FNOR. However, as indicated in Figure 7b by the dotted line for the five Fds that were active in the coupled system, there was a general decrease in V_m with increasing reduction potential. Thus, the lower reduction potential of the Fd variant, the more efficiently it is oxidized by FNOR. The cutoff point for the reaction is quite dramatic (Figure 7b), and falls between −188 mV (for D14V, which was active) and −148 mV (for D14Y, which was inactive).

Thus, as with POR, the reduction potentials of the Fd variants appear to be the primary factor in determining their ability to function as an electron donor to FNOR although, as is expected, the trend with FNOR (Figure 7b) is opposite to that seen with POR (Figure 7a). It is perhaps significant that the WT form of the protein, with Asp 14 and a 4Fe-center, is positioned in the middle of both systems. Thus, it is readily reduced by POR and readily donates electrons to

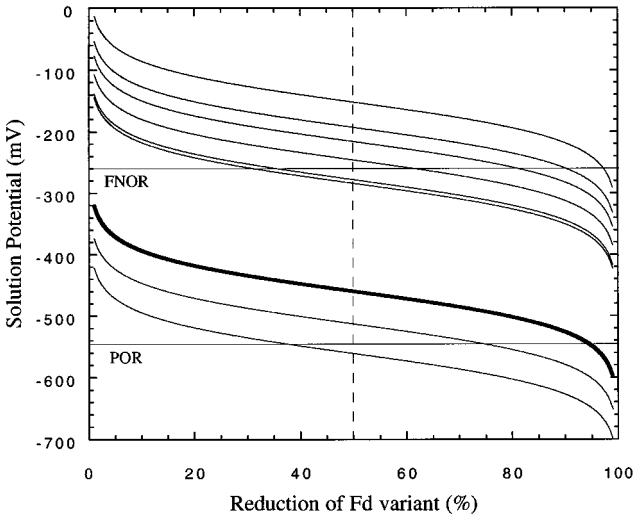

FIGURE 8: Ability of variants of *P. furiosus* ferredoxin to function as electron carriers for pyruvate ferredoxin oxidoreductase and for ferredoxin:NADP oxidoreductase of *P. furiosus* at 80 °C. Nernst plots for the Fd variants are depicted using the reduction potentials measured at 80 °C, pH 7.0 (see Figure 4). The curves represent, from top to bottom, the following Fd forms: 3Fe-D14S, 3Fe-D14N, 3Fe-D14H, 3Fe-D14Y, 3Fe-D14V, 3Fe−WT, 4Fe−WT, 4Fe-D14C, and 4Fe-D14S. The horizontal lines labeled represent the estimated reduction potentials of pyruvate ferredoxin oxidoreductase (POR) and ferredoxin NADP oxidoreductase (FNOR). See text for details.

FNOR. If the reduction potential of the Fd is decreased too much, as with the 4Fe-form of D14S, it is a poor substrate for POR. Indeed, the fact that the 3Fe-form of this mutant exhibited the highest activity emphasizes the effect of potential rather than the nature of residue 14. On the other hand, while the Fd variants with lower reduction potentials than the WT protein, such as the 4Fe-form of D14S, are more active as electron donors to FNOR, those with too positive a potential, such as the 3Fe-form of the same protein, were inactive. The capacity of the various Fds to function as electron carriers with POR and FNOR is illustrated in Figure 8, which depicts a Nernstian-type plot for each Fd. Experimentally it was determined that in the POR assay described above, the extent of reduction of the 4Fe-form of the D14S mutant was only ∼ 40%, while the WT and D14C 4Fe-forms were completely reduced. This suggests a midpoint potential for POR of approximately −520 mV (at 80 °C, pH 8.0), which is lower than that (−450 mV) determined by direct electrochemistry (*45*). Of the six 3Fe-forms examined, the fact that the two with the lowest reduction potentials (WT and D14V) were able to function in the coupled assay (Table 4) indicates a potential for FNOR in the vicinity of −250 mV (80 °C, pH 8.0). Thus, of all the variants examined, Figure 8 indicates that the WT Fd is the most appropriate protein to accept electrons from POR and donate them to FNOR. However, with the range of reduction potentials (∼400 mV) known for biological 4Fe-centers with complete Cys ligation, one wonders why Pf should "choose" Asp coordination for its cluster, especially since incomplete Cys ligation generally leads to cluster instability, that is, Asp substitution is associated with 3Fe- rather than 4Fe-clusters in mesophilic 7Fe-Fds (see, for example, refs *1*−*3*). Perhaps the structural constraints on the Pf Fd protein that impart it with high thermal stability counteract the necessary protein-cluster interactions that would "tune" a 4Fe-center with all Cys coordination in the required redox state. The nature of

those structural constraints, how the reduction potential is tuned, and if the redox-dependent ligation mode of Asp plays a role, are questions yet to be answered.

ACKNOWLEDGMENT

We thank Michael K. Johnson, Frank Jenney, and Angeli Menon for helpful discussions.

REFERENCES

1. Cammack, R. (1992) *Adv. Inorg. Chem. 38*, 281−322.
2. Matsubara, H., and Saeki, K. (1992) *Adv. Inorg. Chem. 38*, 223−280.
3. Johnson, M. K. (1994) in *Encyclopedia of Inorganic Chemistry* (King, R. B., Ed.) pp 1896−1915, John Wiley, New York.
4. Beinert, H., Holm, R. H., and Münck, E. (1997) *Science 277*, 653−659.
5. Beinert, H., and Thomson, A. J. (1983) *Arch. Biochem. Biophys. 222*, 333−361.
6. Heering, H. A., Bulsink, Y. B. M., Hagen, W. R., and Meyer, T. E. (1995) *Biochemistry 34*, 14675−14686.
7. Backes, G., Mino, Y., Loehr, T. M., Meyer, T. E., Cusanovich, M. A., Sweeny, W. V., Adman, E. T., and Sanders-Loehr, J. (1991) *J. Am. Chem. Soc. 113*, 2055−2064.
8. Adman, E. T., Sieker, L. C., and Jensen, L. H. (1973) *J. Biol. Chem. 248*, 3987−3996.
9. Langen, R., Jensen, G. M., Jacob, U., Stephens, P. J., and Warshel, A. (1992) *J. Biol. Chem. 267*, 25625−25627.
10. Jensen, G. M., Warshel, A., and Stephens, P. J. (1994) *Biochemistry 33*, 10911−10924.
11. Conover, R. C., Kowal, A. T., Fu, W., Park, J.-B., Aono, S., Adams, M. W. W., and Johnson, M. K. (1990) *J. Biol. Chem. 265*, 8533−8541.
12. Calzolai, L., Gorst, C. M., Zhou, Z. H., Teng, Q., Adams, M. W. W., and La Mar, G. N. (1995) *Biochemistry 34*, 11373−11384.
13. O'Keefe, D. P., Gibson, K. J., Emptage, M. H., Lenstra, R., Romesser, J. A., Litle, P. J., and Omer, C. A. (1991) *Biochemistry 30*, 447−455.
14. Beinert, H., Kennedy, M. C., and Stout, C. D. (1996) *Chem. Rev. 96*, 2335−2373.
15. Flint, D. H., and Allen, R. M. (1996) *Chem. Rev. 96*, 2315−2334.
16. Peters, J. W., Stowell, S. M., Finnegan, M. A., Johnson, M. K., and Rees, D. C. (1997) *Biochemistry 36*, 1181−1187.
17. Link, T. A., Hagen, W. R., Pierik, A. J., Assmann, C., and von Jagow, G. (1992) *Eur. J. Biochem. 208*, 685−691.
18. Volbeda, A., Charon, M.-H., Piras, P., Hatchikian, E. C., Frey, M., and Fontecilla-Camps, J. C. (1995) *Nature 373*, 580−587.
19. Adams, M. W. W. (1990) *Biochim. Biophys. Acta 1020*, 115−145.
20. Blamey, J. M., and Adams, M. W. W. (1993) *Biochim. Biophys. Acta 1161*, 19−27.
21. Mukund, S., and Adams, M. W. W. (1995) *J. Biol. Chem. 270*, 8389−8392.
22. Mukund, S., and Adams, M. W. W. (1993) *J. Biol. Chem. 268*, 13592−13600.
23. Mai, X., and Adams, M. W. W. (1994) *J. Biol. Chem. 269*, 16726−16732.
24. Mai, X., and Adams, M. W. W. (1996) *J. Bacteriol. 178*, 5890−5896.
25. Heider, J., Mai, X., and Adams, M. W. W. (1996) *J. Bacteriol. 178*, 780−787.
26. Ma, K., and Adams, M. W. W. (1994) *J. Bacteriol. 176*, 6509−6517.
27. Ma, K., Zhou, Z. H., and Adams, M. W. W. (1994) *FEMS Microbiol. Lett. 122*, 245−250.
28. Aono, S., Bryant, F. O., and Adams, M. W. W. (1989) *J. Bacteriol. 171*, 3433−3439.
29. Taniguchi, V. T., Sailasuta-Scott, N., Anson, F. C., and Gray, H. B. (1980) *Pure Appl. Chem. 52*, 2275−2281.
30. Asso, M., Mbarki, O., Guigliarelli, B., Yagi, T., and Bertrand, P. (1995) *Biochem. Biophys. Res. Commun. 211*, 198−204.
31. Soriano, A., Shumin, D. L., Agarwal, A., and Cowan, J. A. (1996) *Biochemistry 35*, 12479−12486.
32. Bertrand, P., Mbarki, O., Asso, M., Blanchard, L., Guerlesquin, F., and Tegoni, M. (1995) *Biochemistry 34*, 11071−11079.
33. Agarwal, A., Li, D., and Cowan, J. A. (1996) *J. Am. Chem. Soc. 118*, 927−928.
34. Heltzel, A., Smith, E. T., Zhou, Z. H., Blamey, J. M., and Adams, M. W. W. (1994) *J. Bacteriol. 176*, 4790−4793.
35. Kunkel, T. A. (1985) *Proc. Natl. Acad. Sci. U.S.A. 82*, 488−492.
36. Sambrook, J., Fritsch, E. F., and Maniatis, T. (1989) *Molecular Cloning: A Laboratory Manual*, Vols 1−3, 2nd ed., Cold Spring Harbor Laboratory Press, Plainview, NY.
37. Zhou, Z. H., and Adams, M. W. W. (1997) *Biochemistry 36*, 10892−10900.
38. Schägger, H., and von Jagow, G. (1987) *Anal. Biochem. 166*, 368−379.
39. Hagen, W. R. (1989) *Eur. J. Biochem. 182*, 523−530.
40. Janz, G. J. (1961) in *Reference Electrodes. Theory and Practice* (Ives, D. J. G., and Janz, G., Eds.) pp 179−230, Academic Press, New York.
41. Verhagen, M. F. J. M., Wolbert, R. B. G., and Hagen, W. R. (1994) *Eur. J. Biochem. 221*, 821−829.
42. Feinberg, B. A., Lo, X., Iwamoto, T., and Tomich, J. M. (1997) *Protein Eng. 10*, 69−75.
43. Calzolai, L., Gorst, C. M., Bren, K. L., Zhou, Z. H., Adams, M. W. W., and La Mar, G. N. (1997) *J. Am. Chem. Soc. 119*, 9341−9350.
44. Dawson, R. M. C., Elliot, D. C., Elliot, W. H., and Jones, K. M. (1986) in *Data for Biochemical Research*, 3rd ed., Oxford University Press, Oxford.
45. Smith, E. T., Zhou, Z. H., Blamey, J. M., and Adams, M. W. W. (1995) *Biochemistry 34*, 7161−7169.
46. Iismaa, S. E., Vazquez, A. E., Jensen, G. H., Stephens, P. J., Butt, J. N., Armstrong, F. A., and Burgess, B. K. (1991) *J. Biol. Chem. 266*, 21563−21571.
47. Moulis, J.-M., and Meyer, J. (1982) *Biochemistry 21*, 4762−4771.
48. Stombaugh, N. A., Sundquist, J. E., Burris, R. H., and Orme-Johnson, W. H. (1976) *Biochemistry 15*, 2633−2641.
49. Lode, E. T., Murray, C. L., and Rabinowitz, J. C. (1976) *J. Biol. Chem. 251*, 1683−1687.
50. Dutton, P. L. (1978) *Methods Enzymol. 54*, 411−435.
51. George, S. J., Richards, A. J. M., Thomson, A. J., and Yates, M. G. (1984) *Biochem. J. 224*, 247−251.
52. Johnson, M. K., Bennett, D. E., Fee, J. A., and Sweeney, W. V. (1987) *Biochim. Biophys. Acta 911*, 81−94.
53. Shen, B., Martin, L. L., Butt, J. N., Armstrong, F. A., Stout, C. D., Jensen, G. M., Stephens, P. J., La Mar, G. N., Gorst, C. M., and Burgess, B. K. (1993) *J. Biol. Chem. 268*, 25928−25939.
54. Park, J.-B., Fan, C., Hoffman, B. M., and Adams, M. W. W. (1991) *J. Biol. Chem. 266*, 19351−19356.
55. Cantor, C. R., and Schimmel, P. R. (1980) *Biophysical Chemistry*, Pt. II, pp 386−389, Freeman and Co., San Francisco.
56. Churg, A. K., and Warshel, A. (1986) *Biochemistry 25*, 1675−1681.
57. Hill, C. L., Renaud, J., Holm, R. H., and Mortenson, L. E. (1977) *J. Am. Chem. Soc. 99*, 2549−2557.
58. Liang, W., and Cowan J. A. (1994) *Inorg. Chem. 33*, 4604−4606.
59. Moulis, J.-M., and Davasse, V. (1995) *Biochemistry 34*, 16781−16788.
60. Calzolai, L., Zhou, Z. H., Adams, M. W. W., and La Mar, G. N. (1996) *J. Am. Chem. Soc. 118*, 2513−2514.

BI972864B